Aperture Theory and the Equivalence Principle

Adriaan J. Booysen

[redacted]

Abstract

Aperture theory in antenna courses is a topic that is usually dealt with fairly superficially at undergraduate and graduate levels. This paper takes a fresh look at aperture theory and its relationship to the Equivalence Principle. Some subtleties and possible misconceptions are discussed. Emphasis is placed on the mathematical analysis of the process by which the aperture is short-circuited, and the subsequent interpretation of various approximations to the aperture fields.

Keywords: Aperture theory; equivalence principle; electromagnetic scattering; electromagnetic coupling; electromagnetic diffraction; image theory; aperture antennas; horn antennas; slot antennas

1. Introduction

Aperture theory [1-3] is a well-known technique used for calculating radiation and scattering from conducting structures with apertures. It is usually employed in conjunction with the Equivalence Principle and various formulations can be applied [1]. In most textbooks, the subject is dealt with rather superficially, and the subtleties are usually not addressed. As a result, the casual reader or student will not be made aware of these unless he or she embarks on an intensive study of the relevant literature. It is the purpose of this paper to revisit some of the techniques we employ, from formulation to practical application.

The following will specifically be addressed:

- Aperture theory is closely related to the Equivalence Principle [1]. A technique often used to simplify calculations is to place a perfect conductor in the null-field region of an equivalence problem [1]. The aperture is then "short-circuited," and one needs to employ only the magnetic current density as a source, since the electric current density effectively cannot radiate in the presence of a conductor. As the remaining magnetic current density now radiates in the presence of the conductor, the impression is created that the free-space radiation integrals can no longer be used to analyze the problem [2, 3]. It will be shown that it is indeed possible to do so by simply applying the Equivalence Principle once more to this new problem. The conductor-in-the-null-region technique will be analyzed mathematically to show exactly what is meant when we state that the electric current density "will not radiate." It will also be shown that we can obtain the same end result (of short-circuited aperture and magnetic source only) by direct manipulation of the free-space radiation integrals. This mathematical analysis shows that the conductor technically has to be placed just within the equivalent surface S, and not coincident with it, as has been suggested [4].
- For aperture antennas with equivalent aperture surface-current densities $\bar{\mathbf{J}}_{ap}$ and $\bar{\mathbf{M}}_{ap}$, the radiated fields are usually calculated from $\bar{\mathbf{J}}_{ap}+\bar{\mathbf{M}}_{ap}$, $2\bar{\mathbf{J}}_{ap}$, or $2\bar{\mathbf{M}}_{ap}$. Discrepancies between the three sets of results are often attributed to the exact aperture fields not being known [5]. It will be shown that differences among the three sets of solutions are related to the choice of the solution, and will exist even if the exact aperture fields were to be known. Several examples will be presented to highlight these differences.

A typical aperture problem is shown in Figure 1a, which depicts the side view of an open-ended waveguide. An internal source, $\bar{\mathbf{J}}$, excites a wave that propagates down the waveguide. Most of the energy of the wave is radiated from the aperture, but a percentage of the energy will be reflected back into the waveguide. From a radiation point of view, however, we are not interested in what happens within the waveguide. To calculate radiation from the aperture, we now proceed to apply the Equivalence Principle to the problem. The Equivalence Principle states that we can replace the physical structure with equivalent electric and magnetic current densities radiating in free space, as long as we retain the sources in the region of interest. For external equivalence, the equivalent current densities will yield the true fields in the external region and null fields within the equivalent surface, S. In Figure 1a, the region of interest is the space external to the waveguide. As there are no sources in this region, we select an equivalent surface, S, tightly enclosing the waveguide and aperture, as shown in Figure 1b.

The waveguide is assumed to be constructed of a perfect electrical conductor, which implies that only an electric current density can exist on its surface. In Figure 1b, we thus have only a $\bar{\mathbf{J}}_{s1}$ on the equivalent conducting surface of the structure, but in the aperture region, we of course have $\bar{\mathbf{J}}_{s1}=\bar{\mathbf{J}}_{ap}$, along with the

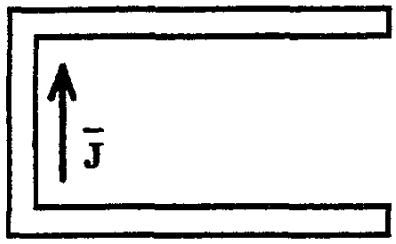

Figure 1a. Aperture-antenna problem solutions: the original problem.

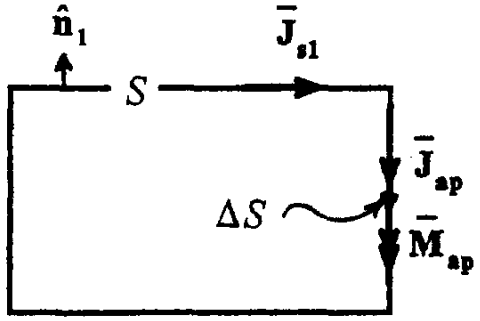

Figure 1b. Aperture-antenna problem solutions: the equivalence solution.

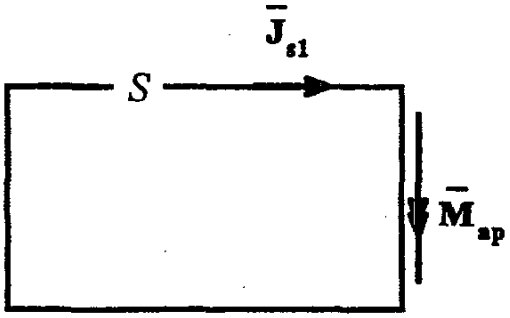

Figure 1c. Aperture-antenna problem solutions: a conductor in null region.

magnetic current density $\bar{\mathbf{M}}_{ap}$. The latter quantities are related to the aperture fields, $\bar{\mathbf{E}}_{ap}$ and $\bar{\mathbf{H}}_{ap}$, through

$$\bar{\mathbf{J}}_{ap} = \hat{\mathbf{n}}_1 \times \bar{\mathbf{H}}_{ap}, \tag{1}$$

$$\bar{\mathbf{M}}_{ap} = -\hat{\mathbf{n}}_1 \times \bar{\mathbf{E}}_{ap}, \tag{2}$$

where $\hat{\mathbf{n}}_1$ is the unit vector normal to S, and $\bar{\mathbf{M}}_{ap} \neq 0$, since the tangential electric field in the aperture is not zero.

The current densities $\bar{\mathbf{J}}_{s1}$, $\bar{\mathbf{J}}_{s1} = \bar{\mathbf{J}}_{ap}$, and $\bar{\mathbf{M}}_{ap}$ in Figure 1b are as yet unknown. For a wide range of aperture problems, however, we know quite well how the aperture fields will behave. We can thus use approximations for $\bar{\mathbf{E}}_{ap}$ and $\bar{\mathbf{H}}_{ap}$, which would allow us to treat $\bar{\mathbf{J}}_{ap}$ and $\bar{\mathbf{M}}_{ap}$ as sources. Keeping in mind that all the current densities radiate in free space, we can then solve for a $\bar{\mathbf{J}}_{s1}$ on the conducting part of the structure by applying the appropriate boundary conditions along the conducting part of S. This technique is what is generally known as "aperture theory."

Although it may sound quite simple, we do not necessarily know the relative distributions of both $\bar{\mathbf{J}}_{ap}$ and $\bar{\mathbf{M}}_{ap}$, as well as their relative magnitudes with respect to each other. The E-field distribution in the aperture can usually be approximated quite accurately (for example, it can be assumed to be either constant or co-sinusoidal across the aperture). The H-field distribution is more difficult to obtain, and it is sometimes almost impossible to calculate the wave impedance in the aperture in a simple way, especially for small apertures such as slots in waveguides. It should be noticed that from the uniqueness theorem, the problem can be solved from knowledge of the tangential E field in the aperture alone [1, pp. 100-103], but we need to solve for the magnetic field in the aperture (and thus $\bar{\mathbf{J}}_{s1} = \bar{\mathbf{J}}_{ap}$) in some way or another.

Before proceeding to look at ways for overcoming this problem, it is instructive to return to the Equivalence Principle for a moment. An elegant mathematical derivation of the Equivalence Principle can be found in [6]. This formulation explicitly requires the Green's functions and surface-current densities to be continuous up to the second derivative everywhere within and on the equivalent surface, S. This requirement originally led the author to believe that the conventional aperture-theory formulation, as discussed above, was mathematically not strictly correct [7]. The argument was that $\bar{\mathbf{M}}_{ap}$ is discontinuous at the aperture edges (zero on the conducting part, non-zero in the aperture), and that the volume enclosed by S must be homogeneous. In the aperture-theory formulation, S encloses a region comprised of conductor and of free space: hence, it would violate the conditions stipulated in [6]. However, this assertion was incorrect. The stipulated conditions apply only to the free-space Green's functions used in the *equivalent solution*, and not to the physical problem. However, the requirement of continuity of the surface-current densities still presents a problem. The normal vector, $\hat{\mathbf{n}}$, is not defined right in the aperture corner (c.f. Figure 1). and there can hence be no gradual change in $\bar{\mathbf{M}}_{ap}$ from a value of 0 on the conductor to some finite value in the aperture.

To be strictly correct in a mathematical sense, one should place the equivalent surface, S, in the free space, just outside, but infinitesimally close to, the physical object. In this case, the same boundary conditions as before can still be applied, but all the fields will be continuous in the free space surrounding the physical object. The only difference is that $\bar{\mathbf{M}}_{ap}$ will extend slightly beyond the aperture corners, but it will decrease very rapidly beyond those points. In practice, there will essentially be no difference, and one can let S coincide with the physical object.

Continuing with the aperture problem shown in Figure 1, we saw that we can replace the physical structure with equivalent current densities radiating in free space, but also that, in most cases, it will still be rather difficult to solve the problem. An ingenious solution was proposed in [1], namely to place a perfect electric or magnetic conductor in the null region (internal to S) of the equivalent problem.

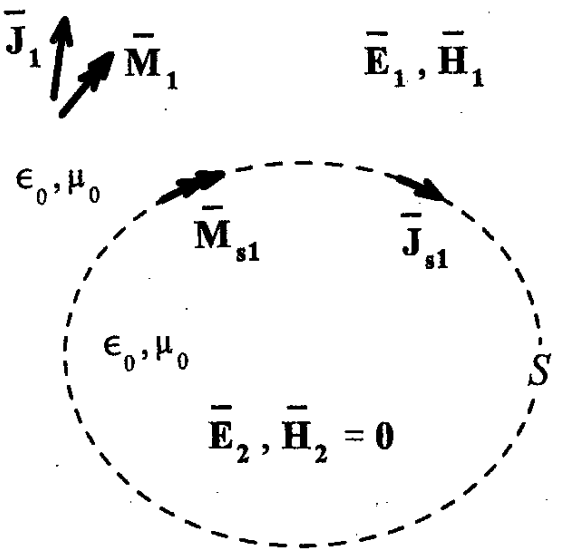

Figure 2a. General equivalence solutions: the general equivalence problem.

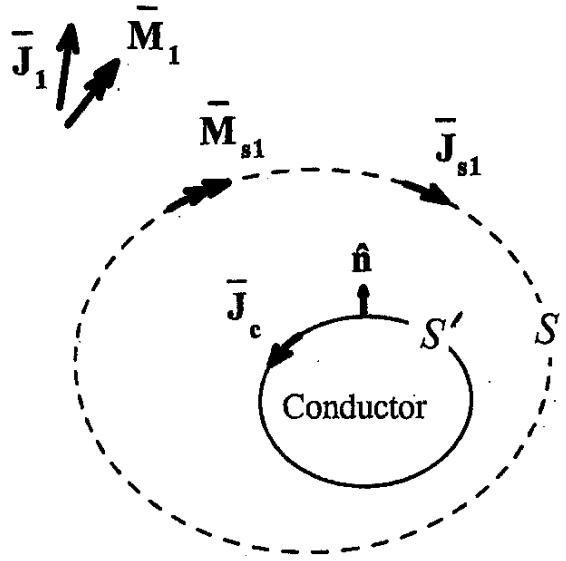

Figure 2b. General equivalence solutions: a conductor placed well within S (new problem).

2. The Placement of Conductors in the Null Field Region of Equivalence Problems

Consider first the general equivalence problem shown in Figure 2. In Figure 2a, the physical scatterer has been replaced by equivalent surface-current densities $\bar{J}_{s1}$ and $\bar{M}_{s1}$, which radiate in free space. The original sources, $\bar{J}_1$ and $\bar{M}_1$, together with the surface-current densities, $\bar{J}_{s1}$ and $\bar{M}_{s1}$, yield the true electromagnetic fields external to S and a null field internal to S. Since there are no fields internal to S, we can place an electric or magnetic conductor within S without influencing the external fields. Figure 2b depicts a conductor as a first step placed well within the null region. The next step is then to expand the conductor until only an infinitesimally small gap is left between the conductor and S. The electric current density $\bar{J}_{s1}$ is now virtually impressed upon a perfect electric conductor, and will effectively not radiate [1]. The electric current density is often referred to as having been "short-circuited," and, as such, can be removed from the problem. Alternatively, one can use reciprocity to show that an electric-current source backed by an electric conductor "will not radiate" [1]. We are then left with the external sources, $\bar{J}_1$ and $\bar{M}_1$, as well as the magnetic current density $\bar{M}_{s1}$, which now radiate in the presence of the conductor. This technique is of special importance in aperture problems, where we usually do not have external sources $\bar{J}_1$ and $\bar{M}_1$.

If we apply the Equivalence Principle as depicted in Figure 2 to the aperture problem shown in Figure 1, the external sources, $\bar{J}_1$ and $\bar{M}_1$, must be removed, and $\bar{J}_{s1}$ and $\bar{M}_{s1}$ will be the current densities due to the sources that were originally in the volume enclosed by S (i.e., within the waveguide). If we now fill the equivalent surface S of this modified Figure 2b with a conductor so that it is located just behind S, $\bar{J}_{s1}$ will be short-circuited everywhere (in Figure 1b, $\bar{J}_{s1}$ on the conducting part of S and $\bar{J}_{s1} = \bar{J}_{ap}$ in the aperture). We will be left with only $\bar{M}_{ap}$ radiating in the presence of a perfect conductor, as shown in Figure 1c. Note that since we placed the conductor just behind S, there will be an infinitesimally small gap between $\bar{M}_{ap}$ and the conductor. Although we seemingly can no longer use the free-space radiation integrals since $\bar{M}_{ap}$ no longer radiates into a homogeneous medium [3], this step is an enormous simplification of the original equivalent aperture problem. Firstly, we no longer need to find $\bar{H}_{ap}$ (and thus $\bar{J}_{ap}$), and secondly, the geometry of the problem has also been simplified significantly. There are many simple geometries for which exact Green's functions can be derived (see, for example, [8] for the detailed characterization of a radiating slot in the broad wall of a waveguide). Once the Green's function for the specific geometry is known, it can be used to calculate the fields radiated by $\bar{M}_{ap}$. As the Green's function represents a conductor, the magnetic current density now radiates in the presence of the conductor.

Apart from examples, the above exposition is more or less what can be found in most textbooks dealing with aperture theory. The rest of this section will deal with the topic in a more detailed manner.

Firstly, it will be shown that one can indeed still use the free-space radiation integrals after having placed a conductor in the null region. Consider again Figure 2b, where we have placed a conductor in the null region of the original equivalence solution. Before we expand the conductor to fill S completely except for an infinitesimally small gap to S, we start off by treating Figure 2b as a brand new problem, in which sources $\bar{J}_1$, $\bar{M}_1$, $\bar{J}_{s1}$, and $\bar{M}_{s1}$ illuminate an electrically conducting body. These current sources will induce a current $\bar{J}_c$ on S', which we now have to determine.

This problem looks just like many other problems we can solve with the Method of Moments (MoM) [9]. In fact, there is nothing preventing us from applying the Equivalence Principle to the new problem once more. We simply replace the conductor with

another equivalent surface, S', with an as-yet-unknown equivalent current density, $\bar{\mathbf{J}}_c$, radiating in free space. We can now expand the equivalent surface, S', until it almost coincides with S. This will then represent the procedure followed by [1], but with all current densities and sources radiating in free space.

We next consider what happens when S' has been expanded so that S' lies just behind S (an infinitesimally small gap separating the two surfaces). In Figure 2b, we can express $\bar{\mathbf{J}}_c$ as

$$\bar{\mathbf{J}}_c = \bar{\mathbf{J}}_c\left(\bar{\mathbf{J}}_1\right) + \bar{\mathbf{J}}_c\left(\bar{\mathbf{M}}_1\right) + \bar{\mathbf{J}}_c\left(\bar{\mathbf{J}}_{s1}\right) + \bar{\mathbf{J}}_c\left(\bar{\mathbf{M}}_{s1}\right). \qquad (3)$$

Since all the electromagnetic fields internal to S are zero and thus $\bar{\mathbf{J}}_c = 0$, all the terms on the right-hand side of Equation (3) must add up to zero, even when S' is infinitesimally close to S. At this stage, one may be inclined to think that placing the conductor in the null region is a futile step, as no current is induced on its surface and it will seemingly have no effect. This is probably the reason why [4] stated that it is incorrect to place the conductor *within* S and that it should rather coincide with S, without a gap separating the two surfaces.

However, when we consider the partial terms of Equation (3) when the electrical conductor (S') has been expanded to nearly fill S, $\bar{\mathbf{J}}_{s1}$ will be infinitesimally close to a conductor, and will induce $-\bar{\mathbf{J}}_{s1}$ on S', i.e., $\bar{\mathbf{J}}_c\left(\bar{\mathbf{J}}_{s1}\right) = -\bar{\mathbf{J}}_{s1}$. Note that this has nothing to do with what we know as "image theory," but will always be the case, irrespective of the shape of S. The negative image of $\bar{\mathbf{J}}_{s1}$ has to be induced in order to maintain the correct boundary conditions on the surface of an electrical conductor. Although $\bar{\mathbf{J}}_{s1}$ will *never* actually stop radiating, radiation from it will effectively be cancelled by radiation from $\bar{\mathbf{J}}_c\left(\bar{\mathbf{J}}_{s1}\right) = -\bar{\mathbf{J}}_{s1}$. This is the only way in which $\bar{\mathbf{J}}_{s1}$ can be "short-circuited." It should be clear that if we now want to remove $\bar{\mathbf{J}}_{s1}$, we actually have to remove the combination of $\bar{\mathbf{J}}_{s1}$ and its image, $\bar{\mathbf{J}}_c\left(\bar{\mathbf{J}}_{s1}\right) = -\bar{\mathbf{J}}_{s1}$. The validity of this step may be debatable, as one is removing the *source* $\bar{\mathbf{J}}_{s1}$, as well as a part of the current that still needs to be solved for. The remaining current densities, $\bar{\mathbf{J}}_c\left(\bar{\mathbf{J}}_1\right) + \bar{\mathbf{J}}_c\left(\bar{\mathbf{M}}_1\right) + \bar{\mathbf{J}}_c\left(\bar{\mathbf{M}}_{s1}\right)$, will then again induce $\bar{\mathbf{J}}_{s1}$ on the conductor, as also recognized by [4] and as shown in Figure 1c.

The practical implication of the above discussion is that we can solve the problem in Figure 1 either by making use of an appropriate Green's function, or we can once more apply the Equivalence Principle and solve the problem by means of the MoM, with all current densities radiating in free space. Even in this case, the aperture will still be "short-circuited," hence considerably simplifying the geometry of the problem, as shown in Figure 1c.

We have now seen that it is indeed possible to use the free-space radiation integrals when the aperture and the original $\bar{\mathbf{J}}_{s1}$ have effectively been "short-circuited." In the next section, a totally different approach will be employed to derive the same result.

3. Short-Circuiting of the Aperture as Derived Directly from the Radiation Integrals

It should be obvious from Figure 1c that we can use either geometry-dependent Green's functions or the free-space radiation integrals to solve the problem, with $\bar{\mathbf{M}}_{ap}$ placed infinitesimally close to, but not coincident with, S. In this section, it will be shown that if one starts off with the original equivalence solution as depicted in Figure 1b, simply moving $\bar{\mathbf{M}}_{ap}$ an infinitesimal distance away from S in accordance with Figure 1c will yield the same result as derived above. Mathematical analysis of this step shows that the aperture appears to have been short-circuited.

Figure 1b shows the Equivalence Principle solution of a typical aperture problem. The segment ΔS represents a small segment of the aperture area. An expanded view of ΔS is shown in Figure 3a. The electric field will initially be evaluated in the aperture region at points just outside and just within the equivalent surface S, shown as points a and c in Figure 3a. The mathematical relationship between various radiation-integral terms will be established, and will then be applied to the case where $\bar{\mathbf{M}}_{ap}$ has been moved away from S, as shown in Figure 3b. In Figure 3, $\bar{\mathbf{M}}_s = \bar{\mathbf{M}}_{ap}$ and $\bar{\mathbf{J}}_s = \bar{\mathbf{J}}_{ap}$. Away from the aperture, $\bar{\mathbf{J}}_s$ represents the current on the conductor $\left(\bar{\mathbf{J}}_s = \bar{\mathbf{J}}_{s1}\right)$ and $\bar{\mathbf{M}}_s = 0$.

Returning to Figure 1b, as discussed before, one can usually find an accurate approximation for $\bar{\mathbf{E}}_{ap}$ (and thus $\bar{\mathbf{M}}_{ap}$), but determining the associated $\bar{\mathbf{H}}_{ap}$ (and thus $\bar{\mathbf{J}}_{ap}$) can be quite a daunting task. One thus cannot readily solve the problem.

If one attempts to treat $\bar{\mathbf{J}}_{ap}$ simply as part of the unknown $\bar{\mathbf{J}}_{s1}$ and sets up a typical MoM solution, one would have to know which boundary conditions to apply in the aperture. For typical two-dimensional problems, one can use the tangential component of $\bar{\mathbf{E}}_{ap}$ in addition to $\hat{\mathbf{n}} \times \bar{\mathbf{E}} = 0$ on the conducting part of S, but $\bar{\mathbf{M}}_{ap}$ as a source first has to be removed by means of non-zero internal (auxiliary) fields [10]. The problem becomes even more difficult for TE problems. Furthermore, from an implementation point of view, the boundary conditions are not uniform on S, which means that one has to keep track over which portions of S which boundary conditions apply. This is not as simple as treating the conducting part as a uniform "scatterer," with the aperture sealed off.

The total electric field at point a in Figure 3a can be expressed as

$$\bar{\mathbf{E}}_a^{tot} = \bar{\mathbf{E}}_a^{tot}\left(\bar{\mathbf{J}}_s, \bar{\mathbf{M}}_s\right) = \bar{\mathbf{E}}_{a,S}\left(\bar{\mathbf{J}}_s\right) + \bar{\mathbf{E}}_{a,S}\left(\bar{\mathbf{M}}_s\right), \qquad (4)$$

where S indicates that the integral is evaluated over the entire contour S. The integrals can be divided into integrals over the sub-contours ΔS and $S - \Delta S$, where ΔS is the sub-contour at point b in Figure 3a. Equation (4) can thus be written as

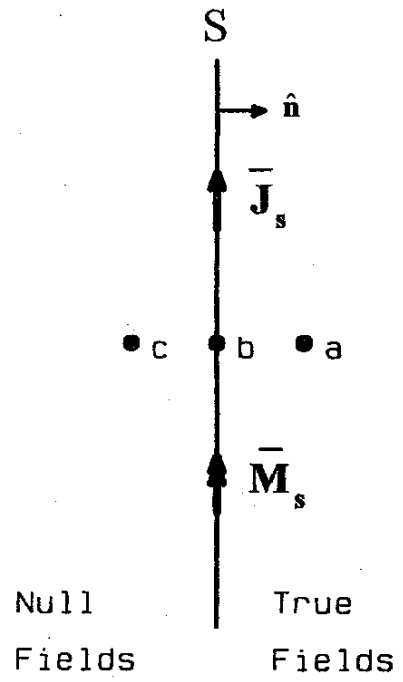

Figure 3a. Field evaluation points in an aperture region: an expanded view of ΔS.

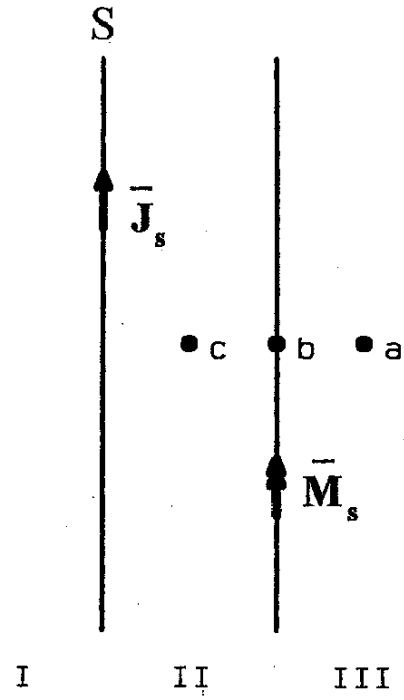

Figure 3b. Field evaluation points in an aperture region: the case where $\bar{\mathbf{M}}_{ap}$ has been moved away from S.

$$\bar{\mathbf{E}}_a^{tot} = \bar{\mathbf{E}}_{a,\Delta S}\left(\bar{\mathbf{J}}_s\right) + \bar{\mathbf{E}}_{a,\Delta S}\left(\bar{\mathbf{M}}_s\right) + \bar{\mathbf{E}}_{a,S-\Delta S}\left(\bar{\mathbf{J}}_s\right) + \bar{\mathbf{E}}_{a,S-\Delta S}\left(\bar{\mathbf{M}}_s\right). \tag{5}$$

As we are dealing with Love's equivalence and since a is infinitesimally close to b, the electric and magnetic equivalent surface-current densities at point b in the aperture region are coincident, and are given by

$$\bar{\mathbf{J}}_s = \hat{\mathbf{n}} \times \bar{\mathbf{H}}_a^{tot}\left(\bar{\mathbf{J}}_s, \bar{\mathbf{M}}_s\right), \tag{6}$$

$$\bar{\mathbf{M}}_s = -\hat{\mathbf{n}} \times \bar{\mathbf{E}}_a^{tot}\left(\bar{\mathbf{J}}_s, \bar{\mathbf{M}}_s\right), \tag{7}$$

where $\hat{\mathbf{n}}$ is the unit vector shown in Figure 3a. From the Appendix, it can be shown that the tangential electric field infinitesimally close to, but just outside, a sub-contour ΔS with an electric-current sheet $\bar{\mathbf{M}}_s$ impressed on it (point a in Figure 3a), is given by

$$\hat{\mathbf{n}} \times \bar{\mathbf{E}}_{a,S}\left(\bar{\mathbf{M}}_s\right) = -\frac{\bar{\mathbf{M}}_s}{2} + \hat{\mathbf{n}} \times \bar{\mathbf{E}}_{a,S-\Delta S}\left(\bar{\mathbf{M}}_s\right). \tag{8}$$

The electric field produced by the integral over the remainder $S - \Delta S$ will be continuous across ΔS, so that

$$\hat{\mathbf{n}} \times \bar{\mathbf{E}}_{c,S-\Delta S}\left(\bar{\mathbf{M}}_s\right) = \hat{\mathbf{n}} \times \bar{\mathbf{E}}_{a,S-\Delta S}\left(\bar{\mathbf{M}}_s\right) \tag{9}$$

and, hence, again using what is shown in the Appendix, we can write

$$\hat{\mathbf{n}} \times \bar{\mathbf{E}}_{c,S}\left(\bar{\mathbf{M}}_s\right) = +\frac{\bar{\mathbf{M}}_s}{2} + \hat{\mathbf{n}} \times \bar{\mathbf{E}}_{a,S-\Delta S}\left(\bar{\mathbf{M}}_s\right). \tag{10}$$

Using Equation (7), Equation (8) can be expressed as

$$\hat{\mathbf{n}} \times \bar{\mathbf{E}}_{a,S}\left(\bar{\mathbf{M}}_s\right) = +\frac{\bar{\mathbf{E}}_{a,\|}^{tot}\left(\bar{\mathbf{J}}_s, \bar{\mathbf{M}}_s\right)}{2} + \hat{\mathbf{n}} \times \bar{\mathbf{E}}_{a,S-\Delta S}\left(\bar{\mathbf{M}}_s\right), \tag{11}$$

where $\bar{\mathbf{E}}_{a,\|}^{tot} = \hat{\mathbf{n}} \times \bar{\mathbf{E}}_a^{tot} = -\bar{\mathbf{M}}_s$ represents the tangential component of the total electric field at point a. We can likewise rewrite Equation (10) as

$$\hat{\mathbf{n}} \times \bar{\mathbf{E}}_{c,S}\left(\bar{\mathbf{M}}_s\right) = -\frac{\bar{\mathbf{E}}_{a,\|}^{tot}\left(\bar{\mathbf{J}}_s, \bar{\mathbf{M}}_s\right)}{2} + \hat{\mathbf{n}} \times \bar{\mathbf{E}}_{a,S-\Delta S}\left(\bar{\mathbf{M}}_s\right). \tag{12}$$

The fields internal to S are identically zero, so that

$$\bar{\mathbf{E}}_c^{tot} = \bar{\mathbf{E}}_{c,S}\left(\bar{\mathbf{J}}_s\right) + \bar{\mathbf{E}}_{c,S}\left(\bar{\mathbf{M}}_s\right) = 0 \tag{13}$$

yields

$$\hat{\mathbf{n}} \times \bar{\mathbf{E}}_{c,S}\left(\bar{\mathbf{J}}_s\right) = +\frac{\bar{\mathbf{E}}_{a,\|}^{tot}\left(\bar{\mathbf{J}}_s, \bar{\mathbf{M}}_s\right)}{2} - \hat{\mathbf{n}} \times \bar{\mathbf{E}}_{a,S-\Delta S}\left(\bar{\mathbf{M}}_s\right) \tag{14}$$

from Equation (12). The tangential electric field produced by $\bar{\mathbf{J}}_s$ is continuous everywhere across S, resulting in

$$\hat{\mathbf{n}} \times \bar{\mathbf{E}}_{a,S}\left(\bar{\mathbf{J}}_s\right) = \hat{\mathbf{n}} \times \bar{\mathbf{E}}_{c,S}\left(\bar{\mathbf{J}}_s\right) = +\frac{\bar{\mathbf{E}}_{a,\|}^{tot}\left(\bar{\mathbf{J}}_s, \bar{\mathbf{M}}_s\right)}{2} - \hat{\mathbf{n}} \times \bar{\mathbf{E}}_{a,S-\Delta S}\left(\bar{\mathbf{M}}_s\right) \tag{15}$$

The total tangential electric field at point a is thus given by the sum of Equations (11) and (15),

$$\begin{aligned} \hat{\mathbf{n}} \times \bar{\mathbf{E}}_a^{tot} &= \hat{\mathbf{n}} \times \bar{\mathbf{E}}_{a,S}\left(\bar{\mathbf{J}}_s\right) + \hat{\mathbf{n}} \times \bar{\mathbf{E}}_{a,S}\left(\bar{\mathbf{M}}_s\right) \\ &= +\bar{\mathbf{E}}_{a,\|}^{tot}\left(\bar{\mathbf{J}}_s, \bar{\mathbf{M}}_s\right), \end{aligned} \tag{16}$$

as expected, while the sum of Equations (12) and (15) yields a null field at point *c*.

Moving on to Figure 3b, where $\bar{\mathbf{M}}_s$ has now been moved an infinitesimal distance to the right of *S*, we now have three regions of interest. The mathematical results derived above still hold, and in Region I the total tangential electric field will be zero. In Region II, the same result is obtained when Equations (12) and (15) are combined, i.e., the total tangential electric field is zero. In Region III, the true non-zero tangential electric field will be obtained.

Since the tangential electric field in Region II is zero, the *entire* surface *S* on which $\bar{\mathbf{J}}_s = \bar{\mathbf{J}}_{ap}$ is imposed can now be thought of as being a perfect electrical conductor. By merely separating $\bar{\mathbf{M}}_s = \bar{\mathbf{M}}_{ap}$ slightly from *S* in an aperture problem we have thus achieved the same result as what was obtained through the process of placing a conductor in the null region. The aperture appears to be "short-circuited" because of the unique relationship between $\bar{\mathbf{J}}_{ap}$, $\bar{\mathbf{M}}_{ap}$, and the radiation integrals. As long as the gap is infinitesimally small, we will be infinitesimally close to the exact solution of the problem.

It is important to note that we cannot argue that when $\bar{\mathbf{M}}_{ap}$ is separated from *S*, the tangential electric field in Region II must be zero because *S* (and thus $\bar{\mathbf{J}}_{ap}$) now represents a conductor. From the Appendix, we know that $\bar{\mathbf{M}}_{ap}$ by itself produces non-zero tangential electric fields on either side of it. With reference to Figure 1b, integration along the entire surface *S*, which includes $\bar{\mathbf{J}}_{s1}$, produces a non-zero tangential electric field just outside *S* in the aperture region. The tangential electric field is produced by $\bar{\mathbf{J}}_{s1}$, $\bar{\mathbf{J}}_{ap}$, and $\bar{\mathbf{M}}_{ap}$, and we have no *a priori* knowledge that $\bar{\mathbf{J}}_{ap}$ will be the same current as what would be the case for a conductor. We have to go through the above derivation to prove that.

The value of this rather complicated derivation is that it clearly shows the interaction of the various radiation-integral terms in this application of the Equivalence Principle, but much more importantly, it shows that there indeed *has to be* a gap between $\bar{\mathbf{M}}_{ap}$ and *S* (in contrast with what was stated in [4]). If this is not the case, we cannot apply the boundary condition $\hat{\mathbf{n}} \times \bar{\mathbf{E}} = 0$ in the aperture region, and we thus cannot regard the aperture as having been short-circuited by a conductor.

We can take the result derived in this section a bit further, by reversing the Equivalence Principle. For the problem shown in Figure 1c, with *S* representing an equivalent surface in free space, we can replace the equivalent surface with a physical conducting surface. Having done that, one can now make use of the appropriate Green's function to solve the problem, if we so prefer. This derivation thus verifies what we have done in Section 3.

In [7], the author presented a somewhat heuristic proof that the aperture can be "short-circuited" in free space, without going through the process of placing a conductor in the null region of the equivalence problem. In [7], both aperture sources $\bar{\mathbf{J}}_{ap}$ and $\bar{\mathbf{M}}_{ap}$ were placed an infinitesimal distance in front of an intentionally "short-circuited" aperture. However, an electric-current density, $\bar{\mathbf{J}}_{ap}$, infinitely close to this planar electric conductor will induce the oppositely directed current, $-\bar{\mathbf{J}}_{ap}$, on the conductor. Radiation from these two terms will always cancel, and will thus have no effect on the total radiation from the structure. One can therefore use only $\bar{\mathbf{M}}_{ap}$ to illuminate the closed surface *S*, which represents a conductor.

4. Apertures in Ground Planes versus Aperture Fields in Free Space

The preceding discussions concentrated on the formulation of aperture antenna problems. In this section, the interpretation of various approximations to the aperture fields will be dealt with. The practical examples presented here were analyzed by means of two-dimensional geometries, representing the E- and H-plane cuts through the physical three-dimensional structures. The patterns calculated in this way are an approximation to the true radiated fields, but will be shown to agree quite closely with the measured results. Invariability with respect to the distance measured perpendicular to each cut was assumed. The E plane is the plane containing the tangential electric field in the aperture and the direction of maximum radiation and, likewise, the H plane is the plane containing the tangential magnetic field in the aperture and the direction of maximum radiation.

Figure 4a depicts a typical planar aperture problem such as a waveguide ending in an infinite ground plane. The Equivalence Principle can be applied to this problem, yielding the equivalent current densities $\bar{\mathbf{J}}_{s1}$, $\bar{\mathbf{J}}_{ap}$, and $\bar{\mathbf{M}}_{ap}$, radiating in free space, as shown in Figure 4b. The electric-current density, $\bar{\mathbf{J}}_{s1}$, exists everywhere along the infinite ground plane, and in the aperture region we have $\bar{\mathbf{J}}_{ap}$ and $\bar{\mathbf{M}}_{ap}$. Figure 4c depicts the equivalence solution in accordance with Section 3 above, with the aperture now having been "short-circuited." It is also the result obtained by placing an electrical conductor in the null region of Figure 4b. Only $\bar{\mathbf{M}}_{ap}$ is regarded as a source, and we have to solve for the unknown $\bar{\mathbf{J}}_s$, where $\bar{\mathbf{J}}_s$ is the combination of $\bar{\mathbf{J}}_{ap}$ and $\bar{\mathbf{J}}_{s1}$ on the conductor. It is generally accepted that one can use any of $\bar{\mathbf{J}}_{s1} + \bar{\mathbf{J}}_{ap} + \bar{\mathbf{M}}_{ap}$, $2\bar{\mathbf{M}}_{ap}$ (an electric conductor placed in the null region, Figure 4c) or $2\left(\bar{\mathbf{J}}_{s1} + \bar{\mathbf{J}}_{ap}\right)$ (a magnetic conductor placed in the null region, not shown) to obtain the electromagnetic fields radiated from the aperture. Collin [5] derived expressions for the gain of an open-ended waveguide, making use of $\bar{\mathbf{J}}_{ap} + \bar{\mathbf{M}}_{ap}$ and $2\bar{\mathbf{M}}_{ap}$. Two different expressions were obtained, the difference being attributed to the exact aperture fields not being known. However, this explanation is not correct.

As the ground plane is infinite, from Figure 4c the induced current $\bar{\mathbf{J}}_s$ represents the image of $\bar{\mathbf{M}}_{ap}$, and we can use $2\bar{\mathbf{M}}_{ap}$ instead of $\bar{\mathbf{J}}_s + \bar{\mathbf{M}}_{ap}$. Whether one thus uses $2\bar{\mathbf{M}}_{ap}$ from Figure 4c or $\bar{\mathbf{J}}_{s1} + \bar{\mathbf{J}}_{ap} + \bar{\mathbf{M}}_{ap}$ from Figure 4b, the same result is achieved. Figure 5 shows the calculated patterns of the X-band open-ended waveguide (aperture height 10.16 mm, width 22.86 mm) in an "infinite" ground plane, as calculated at a radius of 0.8 m using a ground plane of total length 2 m. A distance of 0.8 m is sufficiently far from the aperture for the calculated electromagnetic fields to be regarded as the far-field patterns, whilst reducing the diffraction effects from the edges of the practical ground plane. The induced current, $\bar{\mathbf{J}}_s$, as shown in Figure 4c was calculated by means of the

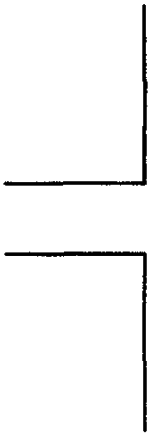

Figure 4a. An aperture in an infinite ground plane: the physical problem.

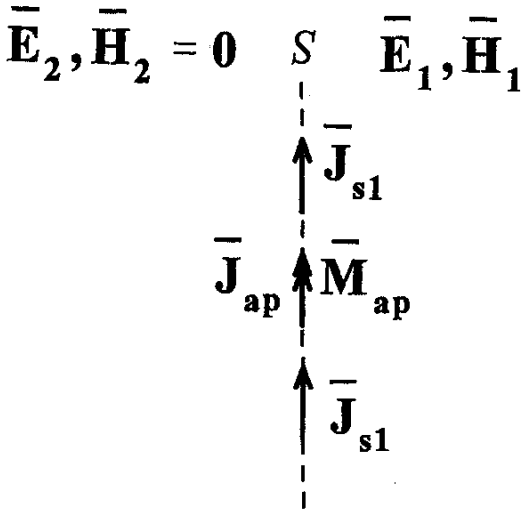

Figure 4b. An aperture in an infinite ground plane: the equivalence solution.

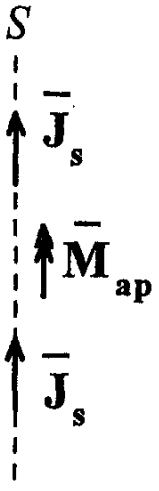

Figure 4c. An aperture in an infinite ground plane: the aperture "short-circuited."

Method of Moments, and $\bar{J}_{ap}$ and $\bar{J}_{s1}$ were simply taken as those portions of $\bar{J}_s$ in the aperture region and on the ground plane, respectively. The frequency was 10 GHz, and $\bar{M}_{ap}$ was assumed to be constant over the aperture and in the direction of the long dimension (22.86 mm) of the aperture. Both $2\bar{M}_{ap}$ and $\bar{J}_{s1} + \bar{J}_{ap} + \bar{M}_{ap}$ give the result A, which is nearly omni-directional. This is to be expected, since an infinitely small aperture in a ground plane would be the dual of an infinitely thin dipole in free space. If one uses only $\bar{J}_{ap} + \bar{M}_{ap}$ instead of $\bar{J}_{s1} + \bar{J}_{ap} + \bar{M}_{ap}$, the result B is obtained. This clearly is the wrong choice, since $\bar{J}_{s1}$ – which exists on the ground plane – cannot be neglected. For an aperture in an infinite ground plane, one should therefore use either $2\bar{M}_{ap}$ or $\bar{J}_{s1} + \bar{J}_{ap} + \bar{M}_{ap}$ (more complicated), but not $\bar{J}_{ap} + \bar{M}_{ap}$.

In the case of an open-ended waveguide in free space with no ground plane present (such as depicted in Figure 1), the situation is different. When we place $\bar{M}_{ap}$ just in front of the sealed-off aperture, as in Figure 1c, we can no longer use image theory to predict the total pattern. Although the $\bar{J}_{ap}$ that will be induced in the aperture region is approximately the same as that in the infinite-ground-plane case, the current on the rest of the structure ($\bar{J}_{s1}$) is significantly different. Curve C shows the pattern of the waveguide of Figure 1, with a total waveguide length of 60 mm and a 1 mm wall thickness (the rectangle in Figure 1c has dimensions 60 × 12.16 mm). In this case, $\bar{J}_{s1}$ falls away rather rapidly on the sides of the waveguide, so that $\bar{J}_{ap} + \bar{M}_{ap}$ should give a fair approximation of the radiation pattern (keep in mind that using $2\bar{M}_{ap}$ would immediately imply that the aperture ends in a ground plane). This is indeed the case, as can be seen from curve B in Figure 5. The pattern calculated from $2\bar{M}_{ap}$ is clearly not accurate. In the case of a waveguide in free space, one should thus use only $\bar{J}_{ap} + \bar{M}_{ap}$ as an approximation.

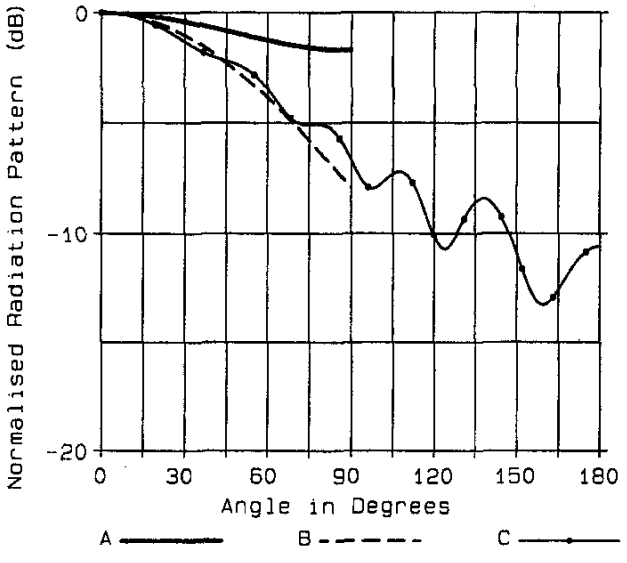

Figure 5. E-plane radiation patterns of a waveguide ending in a ground plane (A) and free space (C). Case A: $\bar{J}_{s1} + \bar{J}_{ap} + \bar{M}_{ap}$ or $2\bar{M}_{ap}$; Case B: $\bar{J}_{ap} + \bar{M}_{ap}$; Case C: Figure 1c.

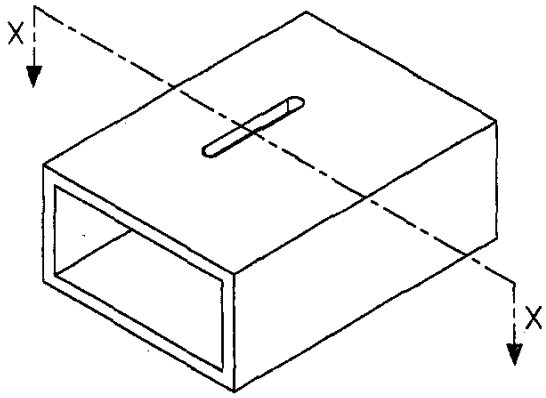

Figure 6a. A section through a broad-wall slot in an X-band waveguide: the physical problem.

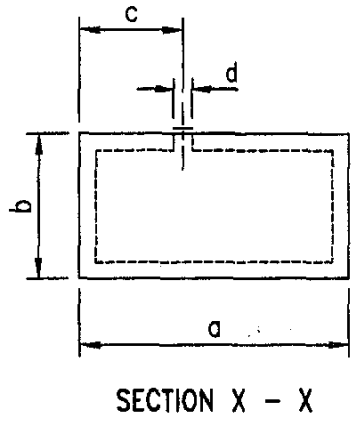

Figure 6b. A section through a broad-wall slot in an X-band waveguide: the two-dimensional equivalent surface (solid line) versus the actual geometry (dashed line); line d is $\bar{\mathbf{M}}_{ap}$.

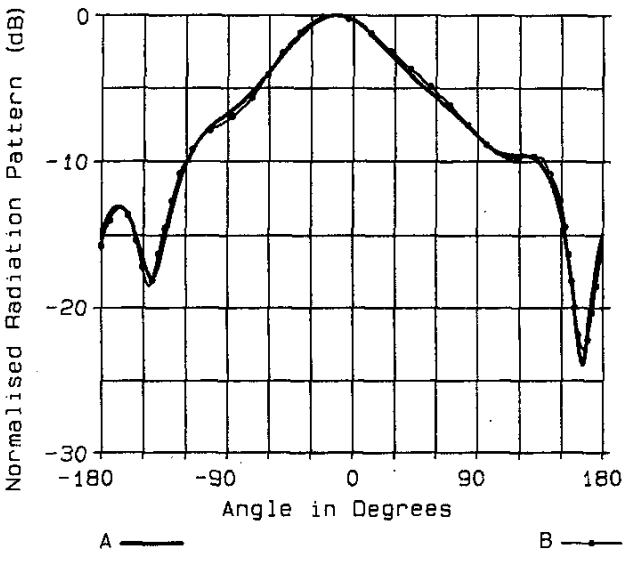

Figure 7. The radiation patterns of an X-band waveguide with a broad-wall slot: (A) calculated; (B) measured.

As a matter of interest, the actual gains of an open-ended waveguide and of a waveguide ending in a large ground plane were both calculated and measured. The calculations were performed for the principal planes only, for two-dimensional structures representing the E-plane and H-plane cuts through the waveguide. The E-plane pattern is shown in Figure 5 (curve C). Linear interpolation between the principal-plane patterns was used to predict the pattern over the rest of the volume. The full three-dimensional pattern was integrated to obtain the directivity. The swept-frequency-measured gains showed moderate ripple as a result of VSWR mismatch, and the "average" curve through the ripple was subsequently taken as the gain. The calculations and measurements yielded a value of about 6.5 dBi for an X-band open-ended waveguide at 10 GHz, and 6.0 dBi for a waveguide ending in a large ground plane. This is to be expected, since the E-plane beamwidth of the waveguide in a ground plane is substantially wider than that of the open-ended waveguide in free space. The formulas given by Collin respectively yield 4.3 dBi ($\bar{\mathbf{J}}_{ap} + \bar{\mathbf{M}}_{ap}$, thus waveguide in free space) and 5.4 dBi ($2\bar{\mathbf{M}}_{ap}$, thus waveguide ending in a ground plane) for the two cases, as discussed above.

It is surprising that the gain in the latter case is higher than in the former case. The simple formula given by [2, Equation (8-70)] yields a gain of 4.2 dBi. The more accurate formulas presented by [11] both give a gain value of 6.5 dBi at 10 GHz for an open-ended waveguide, which confirms the result obtained by means of pattern integration and measurement. The close agreement between the author's theoretical results (linear interpolation between the two-dimensional E- and H-plane patterns) and those of [11] may be a bit fortuitous, as the author did not take the reflection coefficient in the aperture into account, as was done by [11]. A reflection coefficient of magnitude 0.29 at 10 GHz [11] reduces the gain by about 0.4 dB.

When we deal with apertures in electrically small structures, we usually do not have a choice between solutions. An E-plane cut through a slotted X-band waveguide is shown in Figure 6. The E field in the slot aperture was assumed to be constant, and hence $\bar{\mathbf{M}}_{ap}$ is constant. The slot height, d, was 1.8 mm, and the waveguide outer dimensions were $a = 25$ mm and $b = 12$ mm. The distance $c = 10$ mm was measured from the edge of the waveguide to the center of the slot. For a two-dimensional cut, the slot and waveguide lengths were extended longitudinally to $\pm\infty$. The principal E-plane pattern was calculated at 10 GHz using the two-dimensional free-space radiation integrals and the MoM. Figure 7 shows the excellent correlation achieved between the theoretical (A) and the measured (B) patterns. The pattern yielded by $2\bar{\mathbf{M}}_{ap}$ (not shown) is omni-directional to less than a tenth of a dB and is obviously not correct, as it would represent the same aperture in an infinite ground plane.

For electrically large aperture antennas, such as horns or reflector antennas, strictly speaking one should use only $\bar{\mathbf{J}}_{ap} + \bar{\mathbf{M}}_{ap}$, but the aperture fields dominate the radiation pattern to such an extent that $2\bar{\mathbf{M}}_{ap}$ can be used without introducing significant errors into the calculations. This is further illustrated when one considers, as an example, radiation from a two-dimensional E-plane sectoral horn antenna with a large aperture, as depicted in Figure 8. The two-dimensional magnetic radiation integral is given by

$$\bar{\mathbf{H}}(\bar{\mathbf{J}},\bar{\mathbf{M}}) = -\frac{k}{4\eta}\int_s \bar{\mathbf{M}} H_0^{(2)}(kr)\,ds + \frac{k}{4\eta}\int_s (\nabla\cdot\bar{\mathbf{M}})\hat{\mathbf{r}} H_1^{(2)}(kr)\,ds - \frac{jk}{4}\int_s \bar{\mathbf{J}}\times\hat{\mathbf{r}} H_1^{(2)}(kr)\,ds, \quad (17)$$

where r is the distance between the integration and the observation points, and k and η represent the free-space wavenumber and wave impedance, respectively. The vector $\hat{\mathbf{r}}$ is a unit vector in the direction from the integration point to the observation point. For this typical TE_z problem, we can express the aperture current densities as $\bar{\mathbf{M}} = -E_y\hat{\mathbf{z}}$ and $\bar{\mathbf{J}} = -H_z\hat{\mathbf{y}}$, and we also have $\hat{\mathbf{r}} = r_x\hat{\mathbf{x}} + r_y\hat{\mathbf{y}}$. Since $\bar{\mathbf{M}}_{ap}$ is z directed, the divergence term in Equation (17) will be zero.

If we assume the aperture to be wide enough in the H plane so that the wave impedance will be close to the free-space wave impedance, we have $E_y = \eta H_z$. Note that E_y and H_z are not constant across the aperture, but are related to each other by the wave impedance at every point in the aperture.

When we calculate radiation patterns, the observation point is electrically far away from the aperture current densities, and we can thus employ the large-argument forms of the Hankel functions [1, Equation (D-13)] in Equation (17), yielding

$$\bar{\mathbf{H}}(\bar{\mathbf{J}},\bar{\mathbf{M}}) \approx \hat{\mathbf{z}}\frac{k}{4\eta}\sqrt{\frac{2j}{k\pi}}\int_s E_y\frac{e^{-jkr}}{\sqrt{r}}\,ds + \hat{\mathbf{z}}\frac{k}{4\eta}\sqrt{\frac{2j}{k\pi}}\int_s r_x E_y\frac{e^{-jkr}}{\sqrt{r}}\,ds \quad (18)$$

Since the extent of the aperture is small compared with r, r_x in the second integral will only be a function of the far-field observation angle, θ. If θ represents the angle off broadside, $r_x \approx \cos\theta$ and it can thus be removed from under the integral. The contributions from the two integrals are equal only for $\theta = 0°$, corresponding to the broadside direction. As the angle off broadside becomes greater, the contribution from the second integral tends to zero, unlike that of the first integral. It is obvious that if only one of the two surface-current densities is used (multiplied by a factor of two), the resulting radiation pattern will differ from the correct solution given by Equation (18).

For large apertures, the $\cos\theta$ term can be regarded as an "element pattern," while the integral would represent the "array factor" of a large array. As is well known in array theory, the total radiation pattern is given by the product of the array and element patterns. For large arrays, the array factor dominates. For large-aperture antennas, it therefore does not really matter which of the three possible solutions we use. It is only far off the main beam that we will begin to observe differences.

Although the radiated fields will not differ dramatically, we have to be careful when we calculate the gain from the radiation integrals analytically. The two integrals in Equation (18) will clearly have different analytical solutions, and this will also be the case for the three-dimensional radiation integrals. The gain formulas obtained from $\bar{\mathbf{J}}_{ap} + \bar{\mathbf{M}}_{ap}$ and $2\bar{\mathbf{M}}_{ap}$ will thus differ, even if

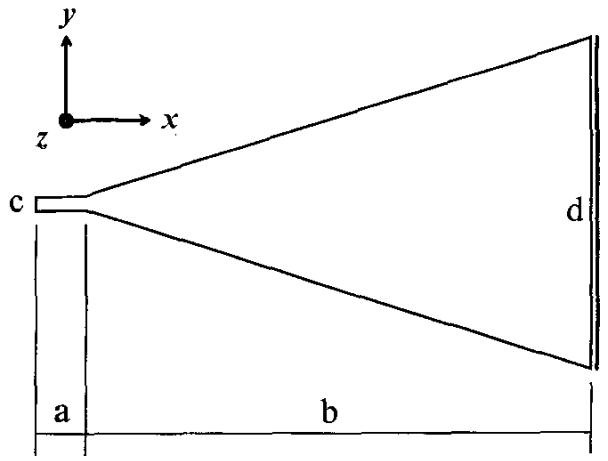

Figure 8. The geometry of an E-plane sectoral horn.

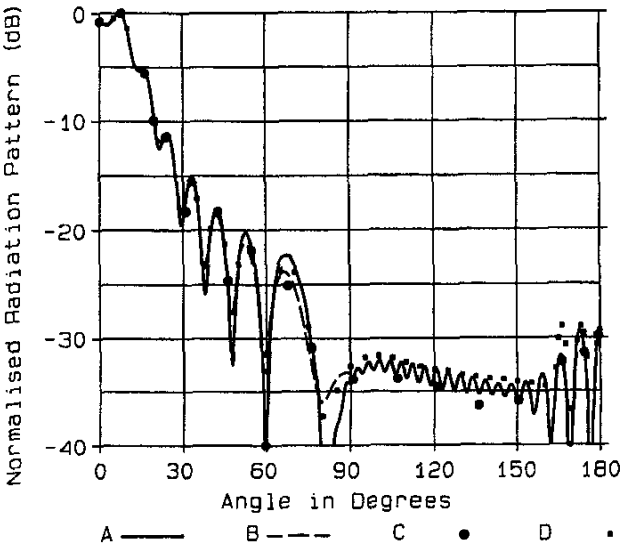

Figure 9. The radiation patterns of an E-plane sectoral horn: (A) calculated; (B) $\bar{\mathbf{J}}_{ap} + \bar{\mathbf{M}}_{ap}$; (C) measured [2]; (D) calculated [2].

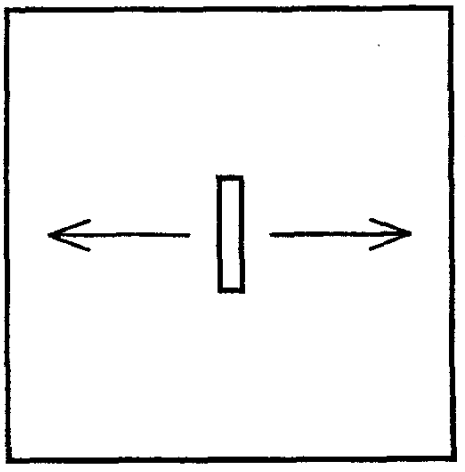

Figure 10. The geometry of a slot in a finite ground plane.

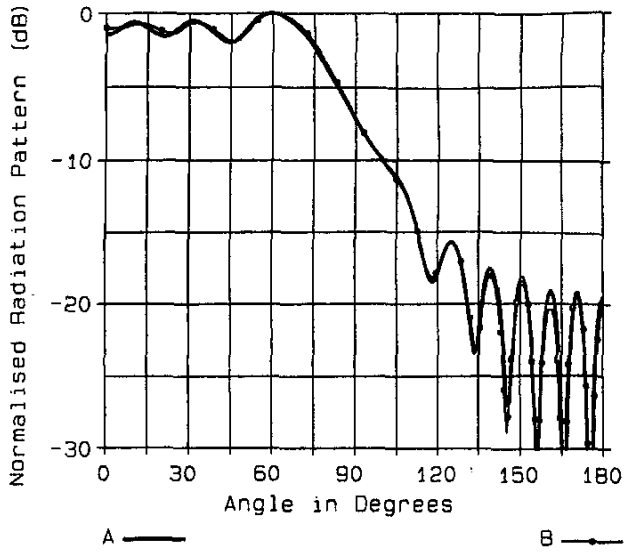

Figure 11. The E-plane radiation patterns for a slot in a finite ground plane: (A) calculated; (B) measured.

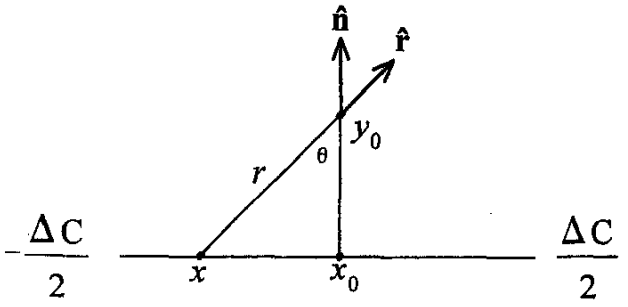

Figure 12. The geometry for the evaluation of the MoM self term.

we happen to know the aperture fields exactly. This is specifically true for electrically small apertures.

When we use the aperture current distributions $\bar{\mathbf{J}}_{ap} + \bar{\mathbf{M}}_{ap}$ to calculate the radiated fields, the results will be valid only in the forward direction. If we are interested in the backward radiation, we have to take the entire structure of the antenna into account. The E-plane sectoral horn antenna shown in Figure 8, with dimensions $a = 36\,\text{mm}$, $b = 370\,\text{mm}$, $c = 12.16\,\text{mm}$, and $d = 244\,\text{mm}$, was analyzed with diffraction theory in [2, Figure 9-21], at a frequency of 10 GHz.

Figure 9 shows the calculated (curve A, by means of the MoM and two-dimensional free-space radiation integrals, aperture "short-circuited," $\bar{\mathbf{M}}_{ap}$ the only source) radiation pattern compared to the pattern given by the sources only (curve B, $\bar{\mathbf{J}}_{ap} + \bar{\mathbf{M}}_{ap}$, from [2, Chapter 8]), the measured data given in [2] (curve C), and the pattern calculated by [2] (curve D). The patterns shown in Figure 9 clearly demonstrate that it is quite sufficient to use only the aperture sources if we are interested in the forward radiation only. It also shows that the two-dimensional representation of a pyramidal horn can yield very accurate principal-plane radiation patterns. The reader is referred to [12] for a detailed analysis of radiation from three-dimensional electrically large horn antennas.

Another example of backward radiation is depicted in Figure 10, where we have a slot of width of 50 mm (half a wavelength at 3 GHz) and a height of 10 mm in the center of a $610 \times 610 \times 4$ mm plate. This problem was analyzed for forward radiation in [2, pp. 485-489], by means of high-frequency techniques. Figure 11 shows the corresponding measured versus calculated E-plane radiation patterns. In the calculations, the tangential electric field was assumed to be constant across the slot, and S was chosen to fully enclose the plate, front and back. The source $\bar{\mathbf{M}}_{ap}$ was placed 0.01λ in front of the solid plate.

For the practical measurements, the slot was fed directly with a coaxial cable. A small rectangular cavity of height 25 mm was placed behind the slot, to limit direct radiation from the slot to the forward region only. Despite poor VSWR, the radiation patterns could still be measured. Copper tape was used to form a trapezoidal structure around the cavity backing the slot. This reduced diffraction from the cavity itself sufficiently for the rear surface of the plate to be treated as planar in the calculations. The correlation between theory and measurement was very good. Note that even though this is a typical "aperture in a ground plane" problem, if we tried to use $2\bar{\mathbf{M}}_{ap}$, the resultant radiation pattern would be omnidirectional in the forward region (0°-90°). The ground plane is simply too small, and diffraction at the ground-plane edges significantly influences the forward and backward radiation patterns of the slot.

Numerous papers have been published dealing with various aspects of aperture problems. The rather complicated approach adopted in [10] was used for calculating the fields radiated from apertures in two-dimensional cylinders. The free-space radiation integrals were also used, as was done in all the examples presented in this paper. Such a complicated approach is not necessary, as one can use the "short-circuit" approach, as discussed above, and depicted in Figure 1c, for both TE_z and TM_z radiation problems. The solution of the problem for both polarizations is obtained in the same way as for typical scattering problems where a conducting object is illuminated by an external source [9, Sections 3.2 and 3.5].

The patterns presented in Figures 4-9 of [10] are easily reproduced by equivalent geometries such as shown in Figure 1c. Calculation of the transmission and reflection coefficients of an aperture in a thick conducting screen is considerably more involved [13, 14], as both the internal and external regions have to be taken into account.

5. Conclusion

The purpose of this paper was to give the reader a better understanding of how the Equivalence Principle can be applied to aperture-antenna problems. Several potential misconceptions appearing in popular antenna-theory textbooks were addressed, the most significant of which being that the free-space radiation integrals cannot be used once a conductor has been introduced in the null region of an equivalence problem. The mathematical analysis and examples presented here hopefully cast a new light upon the well-established techniques used in aperture theory.

6. Acknowledgements

The author wishes to thank Dr. Dirk Baker for helpful discussions, and acknowledges the technical support of Grintek Elec-

tronics during the execution of this work. The author is indebted to Prof. Sembiam Rengarajan who, prior to the submission of the paper, was prepared to correspond with him on the crucial issues of the paper. Even more so, the author is indebted to Prof. Joseph Mautz, who, as a reviewer, was prepared to correspond with him and suggested several improvements.

7. Appendix: Derivation of Moment-Method Self Term

In this Appendix, a mathematical derivation of a "self term," often encountered in Moment Methods, is given. This term is usually derived by considering the discontinuity in the electromagnetic fields above and below the associated equivalent current density [3, p. 713]. It is shown that the radiation integrals themselves also produce this result.

Consider an incremental surface ΔC on the x axis, as depicted in Figure 12. The self term of the EFIE (electric-field integral equation) will be derived here, and it is thus assumed that a TM_z surface current, $\bar{\mathbf{M}}_s = M_t \hat{\mathbf{t}}$, is impressed on this surface, where $\hat{\mathbf{t}}$ is perpendicular to $\hat{\mathbf{n}}$. The integral we wish to evaluate is

$$\hat{\mathbf{n}} \times \bar{\mathbf{E}}(\bar{\mathbf{M}}_s) = \frac{jk}{4} \int_{\Delta C} \bar{\mathbf{M}}_s (\hat{\mathbf{n}} \cdot \hat{\mathbf{r}}) H_1^{(2)}(kr)\, dx . \tag{19}$$

The "self term" is calculated by considering an observation point a distance y_0 above the surface, where $y_0 \to 0$. Since [1, Equations (D-10 and D-12)]

$$H_1^{(2)}(x) \xrightarrow[x \to 0]{} \frac{x}{2} + j\frac{2}{\pi x} \tag{20}$$

and

$$\hat{\mathbf{n}} \cdot \hat{\mathbf{r}} = \cos\theta = \frac{y_0}{\sqrt{(x - x_0)^2 + y_0^2}} = \frac{y_0}{r}, \tag{21}$$

it can be shown that

$$\hat{\mathbf{n}} \times \bar{\mathbf{E}}(\bar{\mathbf{M}}_s) = \frac{jk^2 y_0 \bar{\mathbf{M}}_s}{8} \int_{\Delta C} dx - \frac{\bar{\mathbf{M}}_s}{2\pi} \int_{\Delta C} \frac{y_0\, dx}{(x - x_0)^2 + y_0^2}, \tag{22}$$

where $\bar{\mathbf{M}}_s$ was assumed to be constant over the interval. If $y_0 \to 0$, the first integral in Equation (22) will tend to 0. When the substitution $x - x_0 = x' y_0$ is made in the second integral of Equation (22), the integration boundaries $x_0 \pm \Delta C/2$ correspondingly become $\pm \Delta C/2/y_0$. With ΔC small but fixed and $y_0 \to 0$, the integration boundaries of the second integral in Equation (22) can thus be extended to $\pm\infty$. Recognizing that

$$\int_{-\infty}^{+\infty} \frac{dx}{x^2 + 1} = \pi , \tag{23}$$

it follows that

$$\hat{\mathbf{n}} \times \bar{\mathbf{E}}(\bar{\mathbf{M}}_s) = -\frac{\bar{\mathbf{M}}_s}{2}. \tag{24}$$

If the evaluation point is chosen to be on the opposite side of $\Delta C (y_0 < 0)$,

$$\hat{\mathbf{n}} \times \bar{\mathbf{E}}(\bar{\mathbf{M}}_s) = \frac{\bar{\mathbf{M}}_s}{2}. \tag{25}$$

A similar derivation can readily be done for the three-dimensional radiation integrals.

8. References

1. R. F. Harrington, *Time-Harmonic Electromagnetic Fields*, New York, McGraw-Hill, 1961, pp. 106-112.

2. W. L. Stutzman and G. A. Thiele, *Antenna Theory and Design*, New York, John Wiley & Sons, 1981, pp. 375-385.

3. C. A. Balanis, *Advanced Engineering Electromagnetics*, New York, John Wiley & Sons, 1989, pp. 329-334.

4. J. Appel-Hansen, "Comments on Field Equivalence Principles," *IEEE Transactions on Antennas and Propagation*, **AP-35**, February 1987, pp. 242-244.

5. R. E. Collin, *Antennas and Radiowave Propagation*, New York, McGraw-Hill, 1985, pp. 176-185.

6. K. Chen, "A Mathematical Formulation of the Equivalence Principle," *IEEE Transactions on Microwave Theory and Techniques*, **37**, October 1989, pp. 1576-1581.

7. A. J. Booysen, "Aperture Theory and the Equivalence Theorem," IEEE International Symposium on Antennas and Propagation *Digest*, Orlando, Florida, July 1999, pp. 1258-1261.

8. S. R. Rengarajan, "Compound Radiating Slots in a Broad Wall of a Rectangular Waveguide," *IEEE Transactions on Antennas and Propagation*, **AP-37**, September 1989, pp. 1116-1123.

9. R. F. Harrington, *Field Computation By Moment Methods*, Malabar FL, R. E. Krieger Publishing Co., 1982.

10. R. F. Wallenberg and R. F. Harrington, "Radiation from Apertures in Conducting Cylinders of Arbitrary Cross Section," *IEEE Transactions on Antennas and Propagation*, **AP-17**, 1969, pp. 56-62.

11. A. D. Yaghjian, "Approximate Formulas for the Far Field and Gain of Open-Ended Rectangular Waveguide," *IEEE Transactions on Antennas and Propagation*, **AP-32**, April 1984, pp. 378-384.

12. K. Liu, C. A. Balanis, C. R. Birtcher, and G. C. Barber, "Analysis of Pyramidal Horn Antennas Using Moment Methods," *IEEE Transactions on Antennas and Propagation*, **AP-41**, 1993, pp. 1379-1389.

13. J. R. Mautz and R. F. Harrington, "Boundary Formulations for Aperture Coupling Problems," *AEÜ*, **34**, 1980, pp. 377-384.

14. D. T. Auckland and R. F. Harrington, "A Nonmodal Formulation for Electromagnetic Transmission through a Filled Slot of Arbitrary Cross Section in a Thick Conducting Screen," *IEEE Transactions on Microwave Theory and Techniques*, **MTT-28**, 1980, pp. 548-555.

Introducing the Feature Article Author

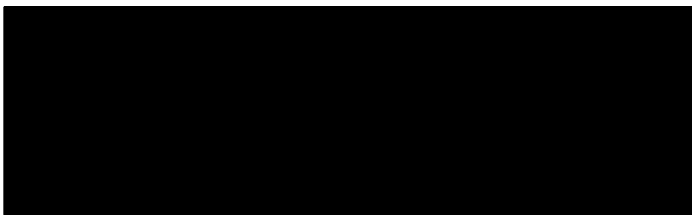

Dr. Booysen has a keen interest in the theoretical aspects of antenna engineering, and has published a couple of technical papers in local and international antenna magazines. He is a past Chapter Chair of the local branch of the IEEE Antennas and Propagation Society.

Editor's Comments *Continued from page 28*

Wireless system engineers sometimes ignore the details of antennas in their systems, simply including the antenna(s) in the channel model. In order to provide such system engineers with a model that can be used in this fashion, while still preserving the important details associated with an antenna, a two-port model for the antenna has been developed. Shawn Rogers, James Aberle, and David Auckland describe their new model in Don Bodnar's Measurements Column. As part of this work, they present a comparison of efficiency measurements made on a planar inverted-F antenna in a spherical near-field range and using the Wheeler-cap method.

Be sure to read Juan Mosig's essay on two notebooks. I think you'll enjoy it.

Instead of the "lite" version of From the Screen of Stone, you get the whole thing this time – and thus there are no "added comments" in these Editor's Comments. A portion of the column deals with Adobe *Acrobat* and the making of PDFs. That should be particularly timely, since the 2004 Symposium in Monterey requires submission in PDF format. The good news is that while you probably want to buy a version of *Acrobat* if you can afford it, you don't have to: there are several ways to make PDFs either for free or at little cost.

The IEEE: Providing a Tool to Help Fight Spam *and* Respecting Our E-mail Rights

Shortly before this issue went to press, I learned that the IEEE was experimenting with software to help identify "spam:" the unsolicited bulk e-mail that has clogged many people's e-mail in-boxes to the point where it seriously affects their ability to use e-mail. As this issue goes to press, a description of the planned implementation can be found at http://eleccomm.ieee.org/IEEE-SPAM-info.shtml. The proposed anti-spam software implementation will read all e-mail sent to or from an IEEE alias account, and if it determines that the e-mail is likely to be spam, it will add "SPAM" (or something similar) to the front of the subject line. This could then be used to visually eliminate such messages, and many e-mail clients will automatically segregate messages so labeled.

I hate spam as much as the next person, and because my e-mail addresses are widely published, I'm a pretty good target. However, I have a real problem with any such process being applied to my e-mail, and particularly without my permission. I think there is a real potential for falsely interfering with legitimate e-mail. I consider it censorship to tamper with e-mail I send or that is sent to me. There is also an issue of trust involved here. Let me expand on these concerns.

First, as I've discussed before in this column (see "Have You Been Filtered Lately" in the December, 2002, issue, pp. 85, 124), I have had several experiences in which commercial spam-filtering software has falsely labeled as spam legitimate messages I have sent to authors of material that was to appear in the *Magazine*. The result was that the timeliness of publication of that material was adversely affected. Had I not gone to extraordinary lengths to get around their spam filtering, the material would never have been published. Published reports have indicated that as much as 15%-20% of legitimate e-mail is being falsely blocked by spam-blocking software. Are you willing to risk losing 20% of your legitimate e-mail? I'm not! [Note: I have no reason to believe – or disbelieve – that such a "false alarm" percentage applies to the system being used by the IEEE. In fact, I've been unable to obtain any data beyond marketing claims on the accuracy rate of any particular spam-blocking software.]

Second, I'm no lawyer, but I consider it libel to falsely label e-mail I have sent as spam. I suspect others probably feel this way, too. I would not want the potential legal liability associated with the use of any system that labeled e-mail as spam unless I was *very* confident it was never going to falsely label a legitimate message.

Third, I consider such labeling to be nothing less than censorship. It is particularly unacceptable since the clear purpose of the modification to the subject line – the tampering with the e-mail – is to allow client e-mail software to reject the message based on the modification. What's next? Deciding what I may or may not send or receive via my IEEE e-mail alias? My understanding of one of the features of the IEEE alias service was that it was to be a simple forwarding service: other than virus checking (which has an almost zero false-alarm rate, and is something everyone sending or receiving e-mail should be doing anyway), there was to be no filtering done by the IEEE. If this had been implemented in the manner originally proposed, any level of trust that the IEEE may have established in the e-mail alias program would have disappeared, at least as far as I'm concerned. I think such a system would be exactly the same as if the US post office started reading mail and changing the address on the letter, based on what someone – or some machine – decided was or was not in the contents, or was or was not acceptable.

I sent some of the above comments to Dan Senese, Executive Director of the IEEE, and had a good telephone conversation with him as a result. He said that the IEEE had been slow to implement any type of spam filtering, in part because they felt some people would have similar concerns. They chose the software they are using because it did not, in and of itself, prevent the delivery of e-mail: it simply labeled it. After checking on the feasibility of

Continued on page 82